





Design of the fractional order internal model controller using the swarm intelligence techniques for the coupled tank system

Sateesh Kumar VAVILALA^{1,*}, Vinopraba THIRUMAVALAVAN¹,
Radhakrishnan THOTA², Sivakumaran NATARAJAN³

¹Department of Electrical and Electronics Engineering, NIT Puducherry, Karaikal, India

²Department of Chemical Engineering, NIT Tiruchirapalli, Trichy, India

³Department of Instrumentation and Control Engineering, NIT Tiruchirapalli, Trichy, India

Received: 02.05.2020

Accepted/Published Online: 31.12.2020

Final Version: 30.03.2021

Abstract: The coupled tank system (comprising two tanks) is used in the chemical industries, water treatment plants etc. Level control of the coupled tank system is a common problem in the process control industry. This work proposes a fractional order internal model controller (FOIMC) with a higher order fractional filter for the level control of the coupled tank system. A first order plus delay time (FOPDT) model of the system is used in the controller design. FOIMC has advantages like robustness to changes in the system gain and extended stability margins. The proposed higher order fractional filter makes the controller physically realizable and quickly roll off the magnitude Bode plot, neglecting the high frequency noise. The particle swarm optimisation (PSO) algorithm is a swarm intelligence based algorithm used for the optimisation problems. The parameters of the FOIMC are optimized with the PSO algorithm by minimizing an objective function constructed using time domain specifications. The novel objective function includes weighted peak overshoot, settling time, and integral square error. A MATLAB (MathWorks, Inc., Natick, MA, USA) based tool, fractional order modelling and control (FOMCON) is used to simulate the fractional order controller. Performance of the proposed FOIMC is compared with two state of the art. Robustness to change in the operating point (tank height) is verified. The proposed FOIMC and the state of the art controllers are implemented on the laboratory setup, and the experimental results are compared.

Key words: Fractional order internal model controller, particle swarm optimisation algorithm, higher order fractional filter, coupled tank system

1. Introduction

This work presents the level control of the cylindrical coupled tank system. In the level control problem, different operating regions have different transfer functions. Hence, the level control of the coupled tank system is an interesting problem. Modeling and control of the cylindrical three tank system using linear quadratic regulator (LQR) is presented in [1]. The coupled system is used in the industry, either in the interacting or in the noninteracting modes [2]. In the interacting mode, the tanks are physically connected by a pipe with valve, and, in the noninteracting mode, the tanks are physically isolated from one another. Among the controllers available for the height control of coupled tank system, internal model controller (IMC) has a single tunable parameter and stable controller [3–4]. The IMC gives better performance for the nonlinear and unstable systems.

*Correspondence: vksateesh@gmail.com

Integer order controllers suffer from disadvantages like less choice in the number of tuning parameters and less robustness. To overcome these difficulties, fractional order controllers are used.

Fractional order controllers are widely used from the last few decades. Podlubny [5] first discussed the fractional order proportional integral derivative (FOPID) controller. The fractional orders of the integrator and differentiator in the FOPID controller give two more tunable parameters to the controller. The fractional order internal model controller (FOIMC) extends the fractional nature to the IMC. The FOIMC combines the advantages of IMC and fractional controllers. [6–7] discussed FOIMC based on the proportional integral derivative (PID) configuration. FOIMC based on the fractional order filter with the analytical design is discussed in [8]. [9–10] discussed implementation of fractional order controller (FOC).

The controller parameter tuning is an important task in the controller design. Parameters of the controller can be tuned using tools like heuristic algorithms, numerical methods, empirical formulae or analytical procedures, and soft computing techniques like neural networks, fuzzy logic, genetic algorithms, etc. Analytical and numerical tuning methods are time consuming and complex, as they depend on the controller's experience and use trial and error based procedure. Of late swarm intelligence algorithm, based controller parameter tuning has become popular. IMC with various combinations of fractional and integer order filters is discussed in [11]. The controller parameters are tuned using an optimisation technique. Some of the recent methods in the FOIMC design are discussed in [12–14]. [12] discussed the design of IMC based on the higher order fractional filter for the two area power system. The tuning is done using GA with ISE as an objective function. Some other industrial and real time applications of the FOC are presented in [15–16]. The implementation of fractional controllers is discussed in [17]. In the present work, the FOMCON toolbox developed by Aleksei Teplajekov [18] is used for implementing the fractional order controller.

The particle swarm optimisation (PSO) algorithm is an example of the swarm intelligence methods. Kennedy and Eberhart proposed the PSO algorithm in 1995 [19]. The PSO algorithm can solve the nonlinear multiobjective type optimisation problems. Even though the PSO algorithm is not a recent technique, it is still effective and used in the controller design. [20] gives the fractional controller design based on PSO. The PSO based digital FOIMC is designed in [21]. PSO algorithm is used to tune the parameters of the FOCs [22–24]. [24] presented a FOPID tuned by PSO algorithm for power systems LFO damping. Integral of time-weighted absolute error (ITAE) is used as an objective function. [25] shows the effect of time domain performance measures on the FOC system design. Smith predictor based FOC is developed in [26]. Fractional controller for the level control problem is discussed in [27]. Time domain specifications of the proposed FOIMC are compared with a fractional order proportional integral (FOPI) controller and FOIMC [28–29]. [30] discussed the design of higher order fractional filter based FOIMC. Along with excellent performance and stability, the controller designed should also have robustness to change in the system parameters and change in the set point. Robust stability can be analyzed analytically using the H_∞ frequency norm of uncertainty [31]. Fragility analysis [32] inspects the robustness to change in the controller parameters using maximum sensitivity M_s . None of the above literature discussed the design of higher order fractional filter based FOIMC, using the PSO algorithm.

Purpose or motivation of the work: [12, 30] discussed the design of IMC based on the higher order fractional filter. The analytical design proposed in [30] is very complex. Motivated by this, the present work proposes a simple tuning process for the IMC based on the higher order fractional filter, using the PSO algorithm.

Main contributions and novelty: The main contributions of this work are designing a higher order fractional filter based FOIMC configuration, hardware realisation of the proposed FOIMC and robustness

verification of the controller to a change in the operating point. The servo tracking and disturbance rejection properties of the proposed controller are verified. The novelty of the present work is a higher order fractional filter based FOIMC configuration, tuned using the PSO algorithm. A novel objective function with time domain specifications is used in the optimisation.

Organisation of the paper: The second section gives the problem formulation of the proposed work. The third section discusses the dynamics of the coupled tank system. From the experimental results, transfer function model of the system is got. In the fourth section, the design, and tuning of the proposed FOIMC are presented. Basics of the PSO algorithm and step by step tuning procedure using PSO algorithm are discussed. In the fifth section, robust stability, gain margin, and fragility of the proposed controller are analytically proven. The fifth section discusses the simulation and experimental results. The sixth section concludes the work.

2. Problem formulation and the proposed methodology

Problem statement: Based on the FOPDT model of the coupled tank system, a controller is designed, which minimizes the desired objective function of the system with a swarm intelligence technique like the PSO algorithm.

Objectives of the controller:

1. The controller should give minimum time domain performance indices.
2. The controller should give satisfactory disturbance rejection and servo tracking.
3. The controller designed should be robust to the changes in the operating point.

In [12], different filter combinations of integer and fractional order, like Eq. (1), (2) are presented.

$$f_2(s) = \frac{1}{(\lambda s + 1)(\gamma s + 1)} \tag{1}$$

$$f_4(s) = \frac{1}{(\lambda s^a + 1)(\gamma s^b + 1)} \tag{2}$$

where λ, γ , are the filter constants and a, b are the fractional orders. A detailed simulation study of the FOIMC with different combinations of the filters is done and the higher order filter given by Eq. (3) gave good integral square error (ISE). Motivated by this, the present work proposes a FOIMC configuration with a higher order fractional filter given by Eq. (3).

$$H(s) = \frac{1}{(1 + \tau_f s^\alpha)^2} \tag{3}$$

Eq. (4) shows the proposed FOIMC based on the higher order fractional filter (Eq. (3)).

$$C_{FOIMC}(s) = \left(\frac{1}{(1 + \tau_f s^\alpha)^2} \right) \left(K_p + \frac{K_i}{s} + K_d s \right) \tag{4}$$

where,

K_p = Gain constant of proportional controller

K_i = Gain constant of integrator

K_d = Gain constant of differentiator
 τ_f = Filter time constant
 α = Fractional order of the filter

Figure 1 shows the proposed FOIMC tuning process with the PSO algorithm. In Figure 1, the plant is a coupled tank system having a FOPDT transfer function model given by Eq. (5).

$$G(s) = \frac{K e^{-Ls}}{Ts + 1} \tag{5}$$

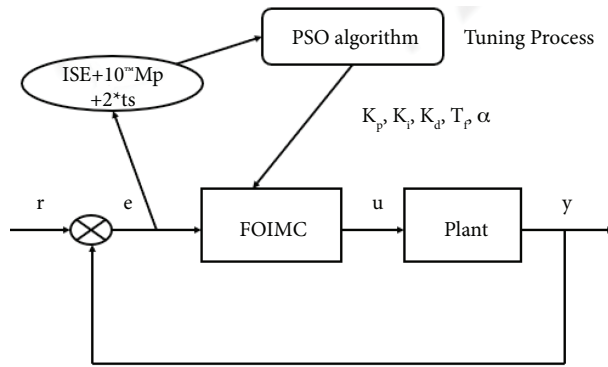


Figure 1. Controller parameters tuning procedure

The coupled tank system has very slow dynamics, hence time domain specifications based tuning is more suitable than the frequency domain specifications. Hence the controller parameters are optimized using the objective function with time domain specifications, peak overshoot (M_p), and time for settling (t_s).

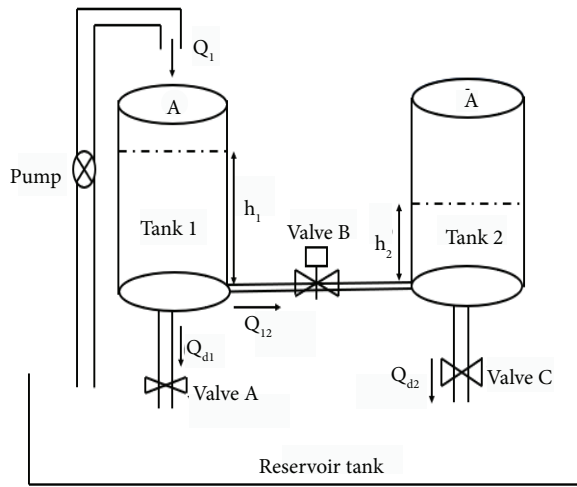
$$J = 10 * M_p + 2 * t_s + \int e^2(t)dt \tag{6}$$

where $e(t)$ is the difference between set point $r(t)$ and output $y(t)$. The weight associated with each term in the objective function changes the priority of that term. M_p , ISE, and t_s are obtained from the response with a step input. The objective function is usually constructed based on the controller objectives. In the level control problem peak over shoot has higher importance, hence it is included with more weight attached to it. ISE reduces the steady state error; hence, it is also included. Settling time affects the integral performance indices like ISE, IAE, ITAE, etc.; hence, it is also included. The weights and additional terms in the objective function are chosen after some experimentation with the execution of the code.

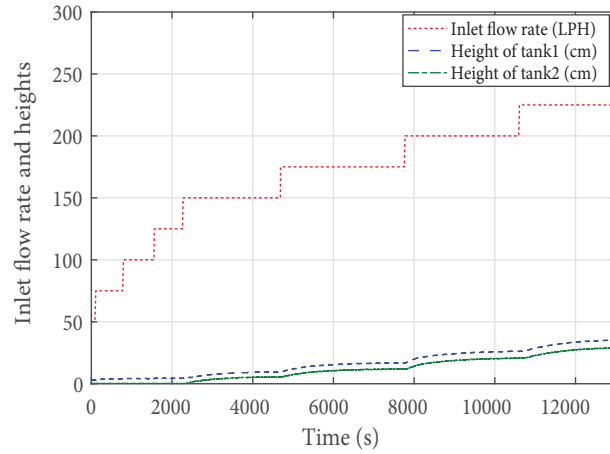
3. Dynamics of the coupled tank system

The coupled tank system connected in the interacting mode is considered in this work. The coupled tank system setup is shown in Figure 2a. Figure 2b shows the open loop test results.

Q_1 = Inlet flow rate
 Q_{12} = Flow rate from the tank one to tank 2
 Q_{d1} = Disturbance flow rate from tank 1



(a) Block diagram of coupled tank system



(b) Open loop test results of the level control

Figure 2. Coupled tank system details

- Q_{d2} = Disturbance flow rate from tank 2
- h_1 = Variable height of the tank 1
- h_2 = Variable height of the tank 2
- D = Diameter of the each tank
- A = Area of each tank

Figure 3a shows the laboratory setup of the coupled tank system. The set up comprises two similar tanks connected via a solenoid valve. The data acquisition (DAQ) card has an analog and digital input and output channels. The DAQ card performs analog to digital signal conversion and interfaces the computer and control panel of the coupled tank system. Reservoir tank stores the water, and the water is pumped to the cylindrical tanks whenever it is needed. The control panel supplies power to the plant and controls the air pressure of different parts. Tank 1 and tank 2 have same physical dimensions. MATLAB/SIMULINK (MathWorks, Inc.) files are run in the computer. The parameters of each tank are given in Table 1. Eq. (7)–(8) represents the dynamics of the coupled tank system.

Table 1. Cylindrical tank parameters.

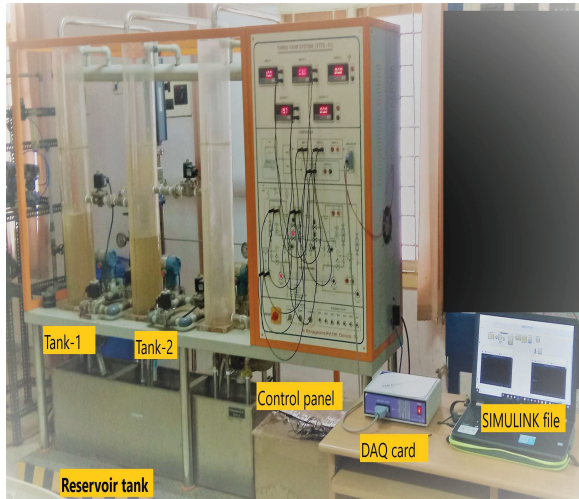
Parameter	H	D	A	Q_{1s}	a_{12}	d	a_{d1}	h_{1s}	h_{2s}	a_{d2}
Value	100 cm	15 cm	176.7 cm ²	175 LPH	0.6	1 cm	0.855	17.5 cm	12.5 cm	0.1839

$$A \frac{dh_1}{dt} = Q_1 - Q_{12}V_2 - Q_{d1} \tag{7}$$

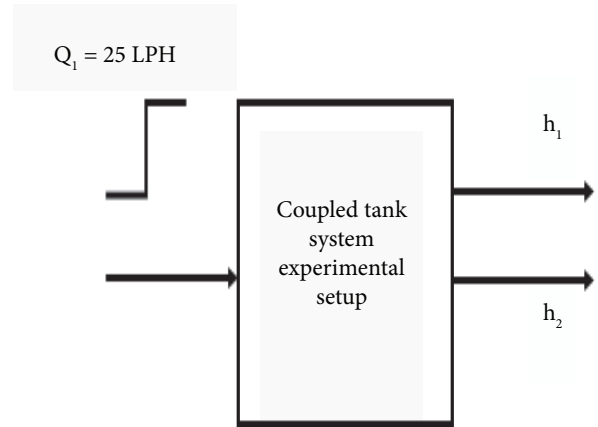
$$A \frac{dh_2}{dt} = Q_{12}V_2 - Q_{d2} \tag{8}$$

The flow rate through the interconnecting solenoid valve B is

$$Q_{12} = a_{12} \text{sign}(h_1 - h_2) \sqrt{2g|h_1 - h_2|} \tag{9}$$



(a) Coupled tank system laboratory setup



(b) Open loop testing block diagram

Figure 3. Experimental details of coupled tank system.

Flow rates through the ball valves A and C are given by

$$Q_{d_1} = a_{d_1} \sqrt{2gh_1} \quad (10)$$

$$Q_{d_2} = a_{d_2} \sqrt{2gh_2} \quad (11)$$

where

a_{d_1} = Coefficient of discharge for valve A

a_{12} = Coefficient of discharge for valve B

a_{d_2} = Coefficient of discharge for valve C

g = Acceleration due to the gravity (98.4 gm/s^2)

V_2 = Valve coefficient of valve B (0 or 1)

d = Diameter of the interconnecting pipe between the tanks

In the operating mode considered, $h_1 \geq h_2$; hence, Eq. (9) reduces to

$$Q_{12} = a_{12} \sqrt{2g(h_1 - h_2)} \quad (12)$$

Substituting Eq. (10)-(12) in Eq. (7), and (8)

$$A \frac{dh_1}{dt} = Q_1 - (a_{12} \sqrt{2g(h_1 - h_2)})V_2 - a_{d_1} \sqrt{2gh_1} \quad (13)$$

$$A \frac{dh_2}{dt} = (a_{12} \sqrt{2g(h_1 - h_2)})V_2 - a_{d_2} \sqrt{2gh_2} \quad (14)$$

Linearising Eq. (13)-(14), around the operating point h_{1s} , h_{2s} , Q_{1s} , using the Taylor series expansion,

$$\begin{aligned}
 A \frac{dh_1}{dt} = & Q_{1s} - (a_{12}\sqrt{2g(h_{1s} - h_{2s})})V_2 - a_{d1}\sqrt{2gh_{1s}} + (Q_1 - Q_{1s}) \\
 & + (h_1 - h_{1s}) \left[-a_{12}\sqrt{2g(1/2)}V_2(h_{1s} - h_{2s})^{-1/2} - a_{d1}\sqrt{2g(1/2)}h_{1s}^{-1/2} \right] \\
 & + (h_2 - h_{2s}) \left[-a_{12}\sqrt{2g(1/2)}V_2(h_{1s} - h_{2s})^{-1/2} \right]
 \end{aligned} \tag{15}$$

$$\begin{aligned}
 A \frac{dh_2}{dt} = & (a_{12}\sqrt{2g(h_{1s} - h_{2s})})V_2 - a_{d2}\sqrt{2gh_{2s}} + (h_1 - h_{1s}) \left[a_{12}\sqrt{2g(1/2)}V_2(h_{1s} - h_{2s})^{-1/2} \right] + \\
 & (h_2 - h_{2s}) \left[a_{12}\sqrt{2g(-1/2)}V_2(h_{1s} - h_{2s})^{-1/2} \right] - \\
 & (h_2 - h_{2s}) \left[a_{d2}\sqrt{2g(1/2)}h_{2s}^{-1/2} \right]
 \end{aligned} \tag{16}$$

At equilibrium, the following relations are obtained:

$$Q_{1s} - (a_{12}\sqrt{2g(h_{1s} - h_{2s})})V_2 - a_{d1}\sqrt{2gh_{1s}} = 0 \tag{17}$$

$$(a_{12}\sqrt{2g(h_{1s} - h_{2s})})V_2 - a_{d2}\sqrt{2gh_{2s}} = 0 \tag{18}$$

Also let us define few constants as,

$$K_1 = \frac{a_{12}\sqrt{2g}(h_{1s} - h_{2s})^{-1/2}V_2}{2A} \tag{19}$$

$$K_2 = \frac{a_{d1}\sqrt{2g}(h_{1s})^{-1/2}}{2A} \tag{20}$$

$$K_3 = \frac{a_{d2}\sqrt{2g}(h_{2s})^{-1/2}}{2A} \tag{21}$$

$$\tilde{h}_1 = h_1 - h_{1s} \tag{22}$$

$$\tilde{h}_2 = h_2 - h_{2s} \tag{23}$$

$$\tilde{Q}_1 = Q_1 - Q_{1s} \tag{24}$$

Using (17)-(24) in (15)-(16),

$$\dot{\tilde{h}}_1 = -\tilde{h}_1(K_1 + K_2) - \tilde{h}_2K_1 + (\tilde{Q}_1/A) \tag{25}$$

$$\dot{h}_2 = \tilde{h}_1 K_1 - \tilde{h}_2 (K_1 + K_3) \quad (26)$$

Taking Laplace transforms on both the sides of Eq. (25)-(26),

$$sH_1(s) = -H_1(s)(K_1 + K_2) - H_2(s)K_1 + (Q_1(s)/A) \quad (27)$$

$$sH_2(s) = H_1(s)K_1 - H_2(s)(K_1 + K_3) \quad (28)$$

By solving Eq. (27)-(28), the transfer function, $G(s) = H_2(s)/Q_1(s)$ is obtained as,

$$G(s) = \frac{K_1/A}{s^2 + (2K_1 + K_2 + K_3)s + K_1^2 + (K_1 + K_3)(K_1 + K_2)} \quad (29)$$

In the present work, the operating region of the level control is selected as (5–15) cm. By substituting parameters of the system from Table 1 into Eq. (29), the analytical model of the system is obtained as

$$G(s) = \frac{6X10^{-5}}{s^2 + 0.0313s + 0.236X10^{-3}} \quad (30)$$

Figure 3b shows the block diagram of open loop testing process, which is useful to get the system transfer function. From the experimental setup, open loop test results are obtained by varying the inlet flow rate Q_{1s} from (50–225) LPH in steps of 25 LPH. Each change of inlet flow rate by 25 LPH corresponds to a step input of 25 units magnitude. Steady state heights of tank 1 and tank 2 corresponding to each change of inlet flow rate, are recorded. Figure 2b shows the plots of variations in inlet flow rate, and the corresponding change in heights of tank 1 and tank 2 separately. But the open loop input and output data (Fig. 2b) shows that a first order FOPDT model (in the (5–15) cm range) given by Eq. (31) is sufficient. The FOIMC is designed based on this FOPDT transfer function model.

$$G(s) = \frac{0.268e^{-10s}}{975s + 1} \quad (31)$$

4. Design of the FOIMC

4.1. Fundamentals of IMC

IMC is based on the model of the plant. The block diagram shown in Figure 4a illustrates IMC.

$R(s)$ = Reference input

$C(s)$ = Feedback controller transfer function

$U(s)$ = Controller output

$Q(s)$ = IMC controller transfer function

$G(s)$ = Plant transfer function

$d(s)$ = Disturbance at the output side

$Y(s)$ = Plant output

\tilde{Y} = Output of the model

$E(s)$ = Error signal

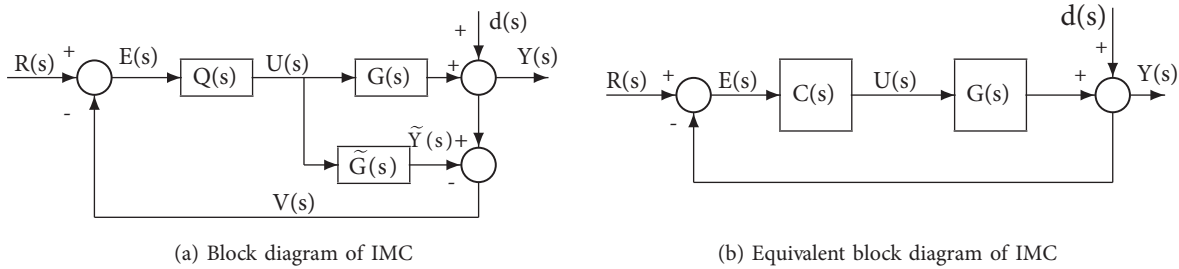


Figure 4. IMC block diagrams

$$V(s) = Y(s) - \tilde{Y}(s)$$

$$\tilde{G} = \text{Model of the plant}$$

The equivalent block diagram of Figure 4a is shown in Figure 4b. Eq. (32) shows the relation between $C(s)$ and $Q(s)$ (assuming that the plant transfer function and model of the plant are same).

$$C(s) = \frac{Q(s)}{1 - Q(s)\tilde{G}} \quad (32)$$

The filter term $H(s)$ is important tunable component in the FOIMC. The higher order of the fractional filter makes the controller physically realizable and gives quick roll off of the magnitude curve in the frequency domain and eliminates the high frequency noise. The presence of the integer order integrator in the C_{FOIMC} , ensures zero steady state error.

Advantages of the proposed FOIMC:

1. Robustness to system gain variations or isodamping property.
2. Infinite gain margin.
3. Increased stability range.

4.2. PSO basics and FOIMC optimisation

The PSO algorithm is widely used in the constrained/unconstrained optimisation problems. The PSO algorithm is used to tune the FOIMC parameters. In the PSO algorithm, the particle's position and particle's velocity are governed by Eq. (33)–(34).

$$V_i(p + 1) = w * V_i(p) + c_1(p_i(p) - x_i(p)) + c_2(g(p) - x_i(p)) \quad (33)$$

$$x_i(p + 1) = x_i(p) + V_i(p + 1) \quad (34)$$

where,

$V_i(p)$ = Velocity of the particle at instant p

$V_i(p + 1)$ = Velocity at the instant $(p + 1)$

w = Weight

c_1 = Cognitive learning constant

c_2 = Social learning constant

$g(p)$ = Globally best value

$p_i(p)$ = Particle's best value

$x_i(p)$ = Particle's position at p

$x_i(p + 1)$ = Particle's position at $(p + 1)$

The FOIMC design process used in this work, with the PSO algorithm is summarized in the following steps:

1. Obtain the FOPDT model of the system.
2. Select appropriate upper and lower bounds for the controller parameters.
3. Construct the objective function to be minimised based on the controller objectives.
4. Choose proper parameters for the PSO algorithm.
5. Obtain the controller parameters after execution of the MATLAB (MathWorks, Inc.) code for the PSO algorithm.
6. Simulate the controller using SIMULINK and check the step response of the closed loop system.
7. Repeat Step 2 to Step 6 with necessary modifications until desired step response is obtained.

Figure 5a shows the flowchart of the PSO algorithm. Figure 5b shows the convergence of the objective function, J using the PSO algorithm. Details of the PSO algorithm are given in Table 2. The PSO algorithm is run several times to check for consistency of the execution. Table 3 gives the statistical analysis of 50 runs of the PSO algorithm. The variation of the FOIMC parameters during the execution of the PSO algorithm for the best run is given in Figure 6.

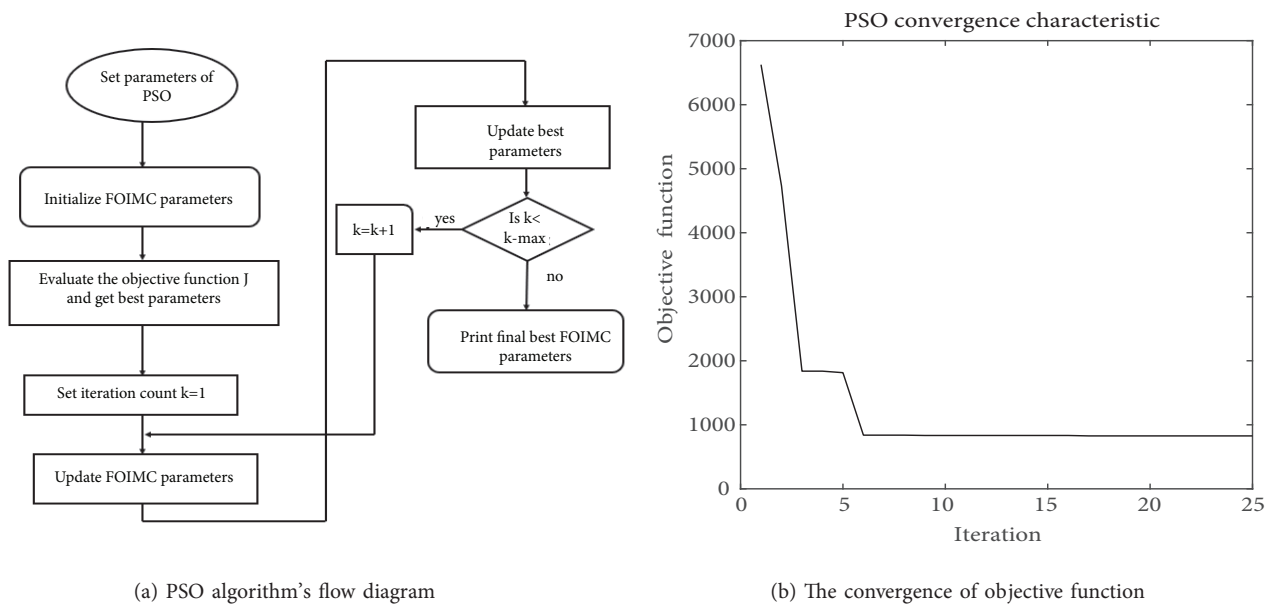


Figure 5. PSO characteristics.

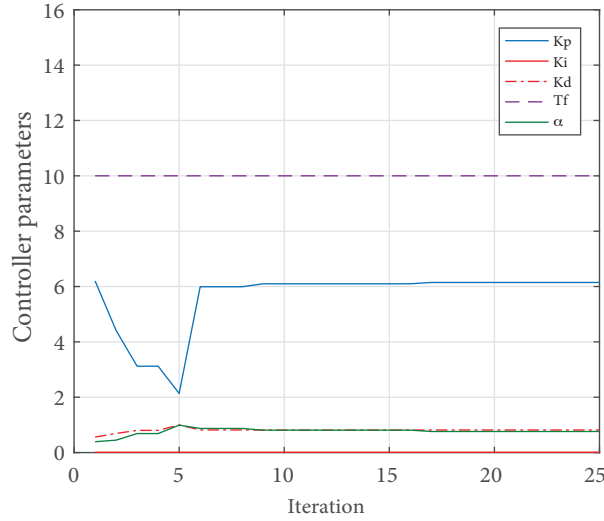


Figure 6. Variation of FOIMC parameters during PSO algorithm execution

Table 2. Details of the PSO algorithm

Parameter	No. of iterations	No. of runs	c_1	c_2	Swarm size	ω_{max}	ω_{min}
Value	25	50	2	2	10	0.9	0.4

Upper and lower bounds of the FOIMC controller parameters used in the MATLAB (MathWorks, Inc.) coding for the PSO algorithm are shown in Eq. (35).

$$\begin{aligned}
 1 &\leq K_p \leq 10 \\
 0.01 &\leq K_i \leq 1 \\
 0.1 &\leq K_d \leq 1 \\
 0.1 &\leq \tau_f \leq 10 \\
 0.01 &\leq \alpha \leq 1
 \end{aligned} \tag{35}$$

4.3. Robust stability analysis

To support the claims of the robustness, stability and gain margin of the proposed higher order filter based FOIMC, an analytical study is presented. The designed controller has to perform reasonably well for a change in the operating point. The closed loop system is robustly stable for a change in the operating point, if the following stability H_∞ norm inequality is satisfied [31].

$$20 \times \log_{10}(|T_C(j\omega)||G_\Delta(j\omega)|) < 0dB \tag{36}$$

Where $T_C(s)$ is the complementary sensitivity transfer function of the closed loop system.

$$T_C(s) = \frac{G(s)C(s)}{1 + G(s)C(s)} \tag{37}$$

Expanding the system transfer function $G(s)$ using Taylor series of first order,

$$G(s) = \frac{-KLs + K}{Ts + 1} \quad (38)$$

Substituting Eq. (4) and (38) in Eq. (37), and simplifying,

$$T_C(s) = \frac{\left(\frac{-KLs+K}{Ts+1}\right)\left(\frac{1}{(1+\tau_f s^\alpha)^2}\right)\left(K_p + \frac{K_i}{s} + K_d s\right)}{1 + \left(\frac{-KLs+K}{Ts+1}\right)\left(\frac{1}{(1+\tau_f s^\alpha)^2}\right)\left(K_p + \frac{K_i}{s} + K_d s\right)} \quad (39)$$

Let the transfer function of the system at a different operating point be,

$$G_1(s) = \frac{K_1 e^{-L_1 s}}{T_1 s + 1} = \frac{-K_1 L_1 s + K_1}{T_1 s + 1} \quad (40)$$

Uncertainty in the plant transfer function $G_\Delta(s)$ is defined as

$$G_\Delta(s) = \frac{G_1(s) - G(s)}{G(s)} \quad (41)$$

Substituting Eq. (38) and (40) in Eq. (41), $G_\Delta(s)$ is obtained as shown in Eq. (42).

$$\frac{(KLT_1 - K_1 L_1 T)s^2 + (K(L - T_1) - K_1(L_1 - T))s + K_1}{-KLT_1 s^2 + (KT_1 - KL)s + K} \quad (42)$$

4.4. Fragility analysis

Apart from robustness to system parameter variation, robustness to controller parameter variation needs attention. While analog controller implementation suffers from physical parameter changes [32], digital controller implementation suffers from the inaccuracies in fixed word length and round offs in numerical calculation. The robustness of the controller parameter variation is analyzed using fragility index $RFI_{\Delta 20}$ [32] defined by Eq. (43).

$$RFI_{\Delta 20} = \left| \frac{M_{S\Delta 20}}{M_S} - 1 \right| \quad (43)$$

where M_S is the nominal maximum sensitivity and $M_{S\Delta 20}$ is the nominal maximum sensitivity obtained when all the controller parameters are varied by +20%. The controller is said to be resilient to controller parameter changes, for values of the $RFI_{\Delta 20} \leq 0.1$; it is nonfragile for values of $0.1 < RFI_{\Delta 20} \leq 0.5$ and fragile for values of $RFI_{\Delta 20} > 0.5$.

4.5. Gain margin analysis

If the gain margin is more, then the system is more stable. The gain margin GM depends on the magnitude of the loop transfer function $G(j\omega)C(j\omega)$.

$$GM = \frac{1}{|G(j\omega)C(j\omega)|} \quad (44)$$

Consider $C_1(s)$ a lower order fractional filter based FOIMC, and $C_2(s)$ a higher order fractional filter based FOIMC. GM_1 is the gain margin of the system with $C_1(s)$ as controller, and GM_2 is the gain margin of the system with $C_2(s)$ as the controller.

$$C_1(s) = \left(\frac{1}{1 + \tau_f s^\alpha} \right) \left(K_p + \frac{K_i}{s} + K_d s \right) \quad (45)$$

$$C_2(s) = \left(\frac{1}{(1 + \tau_f s^\alpha)^2} \right) \left(K_p + \frac{K_i}{s} + K_d s \right) \quad (46)$$

From Eq. (44), a proportionality can be written as $GM \propto \frac{1}{|C(j\omega)|}$. Hence GM_1 and GM_2 can be rewritten as,

$$GM_1 \propto \frac{1}{|C_1(j\omega)|} \quad (47)$$

$$GM_2 \propto \frac{1}{|C_2(j\omega)|} \quad (48)$$

From Eq. (47) and (48), taking out the common terms

$$GM_1 \propto |1 + \tau_f s^\alpha| \quad (49)$$

$$GM_2 \propto |(1 + \tau_f s^\alpha)^2| \quad (50)$$

From Eq. (49) and (50) always $GM_2 > GM_1$, which proves that a higher order fractional filter based FOIMC will have a higher gain margin compared to lower order fractional filter based FOIMC.

5. Results and discussion

The parameters of the FOIMC are obtained using the PSO algorithm coded in MATLAB (MathWorks, Inc.). For the coupled tank system with the transfer function [31], the proposed FOIMC is obtained as,

$$C_{FOIMC}(s) = \frac{1}{(1 + 10s^{0.762})^2} \left(6.14 + \frac{0.01}{s} + 0.816s \right) \quad (51)$$

To verify the effectiveness of the proposed FOIMC its performance is compared with two state of the art controllers [28–29]. Using the frequency domain specifications as phase margin (PM) = 30°, gain crossover frequency (GCF) = 0.001 rad/sec, the FOIMC (Ref-1) [28] is obtained as,

$$C_{FOIMC-Ref-1}(s) = \frac{975s + 1}{0.268(14.39s^{1.23} + 10s)} \quad (52)$$

FOPI controller (Ref-2) [29] for the coupled tank system is obtained using the gray wolf optimisation (GWO) algorithm as,

$$C_{FOPI-Ref-2}(s) = 15.37 + \frac{1.29}{s^{0.845}} \quad (53)$$

The results of the proposed controller are also compared with an integer order IMC, with a higher order filter.

$$Q_{IOIMC}(s) = \frac{1}{(1 + 10s)^2} \left(\frac{1 + 975s}{0.268} \right) \tag{54}$$

Using Eq. (32) C_{IOIMC} is obtained as,

$$C_{IOIMC}(s) = \frac{3638s + 3.73}{100s^2 + 30s} \tag{55}$$

Table 3. Statistical analysis of PSO runs

Parameter	Best	Worst	Mean	Standard deviation
Objective function (J)	826.55	20008	2437.6	3290.8

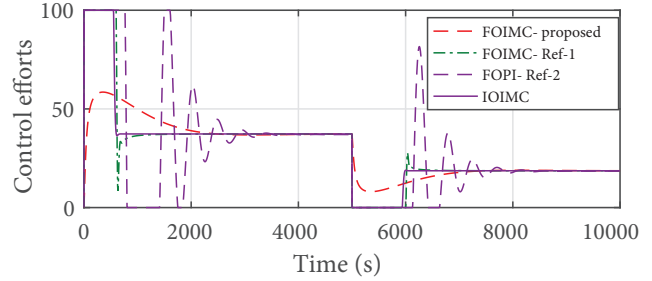
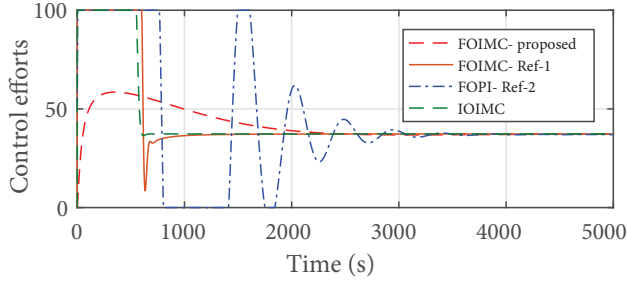
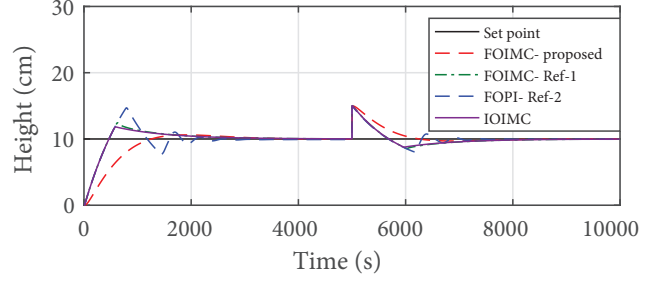
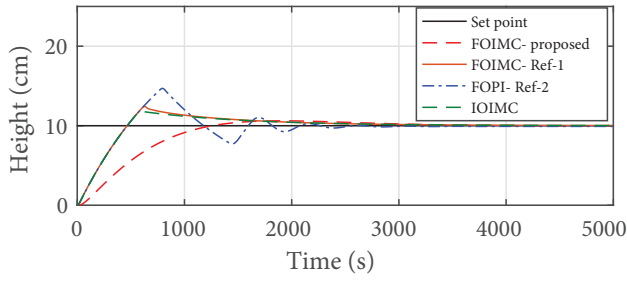
MATLAB/SIMULINK (MathWorks, Inc.) and the FOMCON toolbox are used to implement the FOIMC. The FOMCON toolbox provides the fractional transfer function, FOPID controller blocks in the SIMULINK. The sampling time used during the simulation is 0.01 s. It is desired to change the height of the second tank from 0 to 10 cm; hence, a step input of magnitude 10 is given during the simulation. Figure 7a shows the step responses and control efforts of the controllers. Table 4 compares the time domain specifications of the controllers got from the step responses. From Table 4 it is observed that peak overshoot is the least for the proposed FOIMC. The physical system in real time has a saturation of 0 to 100% in the controller output. Control efforts show the energy consumed in obtaining the desired control action. Figure 7a shows that FOIMC consumes less control energy. The proposed FOIMC has control effort, well within the saturation limits, and control efforts of other controllers are hitting the saturation limits.

Regulatory responses show the disturbance rejection property of the controller. Figure 7b compares the regulatory responses and the corresponding control efforts. A disturbance of 5 cm is given at 5000 s, and the regulatory responses are obtained. The FOIMC rejects the disturbance and settles quickly to 10 cm level. The servo responses show the tracking ability of the controller with time varying set point. A step vector of [5 15] cm is given at a time vector of [0 5000 10000] s. Figure 8a shows the servo responses. Both the servo and regulatory responses of the proposed FOIMC are better than the responses of other controllers.

$$\frac{h_2(s)}{q_{in}(s)} = \frac{0.3e^{-20s}}{1095s + 1} \tag{56}$$

There will be a certain amount of uncertainty associated with the modelling of the parameters of the system. As time progresses because of wear and tear, the parameters of the system get altered. So, the controller designed should take care of these uncertainties and be robust enough to the parameter changes. In this work, the controller’s robustness is verified by operating it in an adjacent operating region of (16–30) cm. The transfer function of the new region is Eq. (56) and the new set point is 20 cm. The corresponding robustness results of the controllers are shown in Figure 8b. All the controllers showed satisfactory robustness. There is no drastic change in the performance of the controllers with a change in the system transfer function.

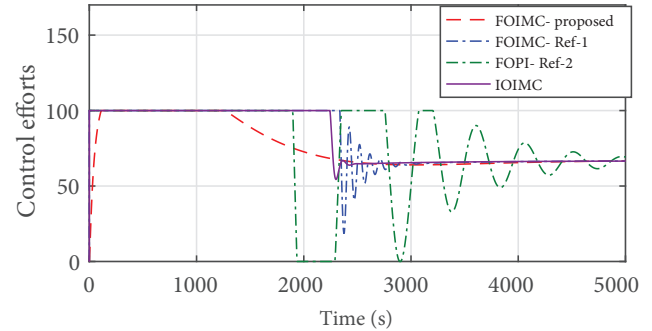
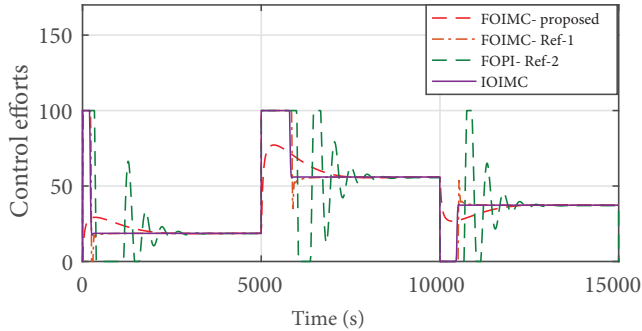
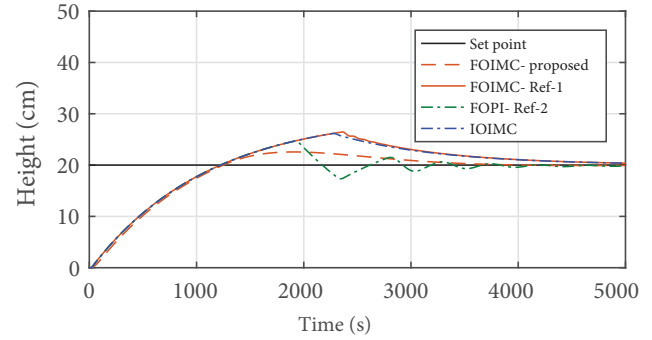
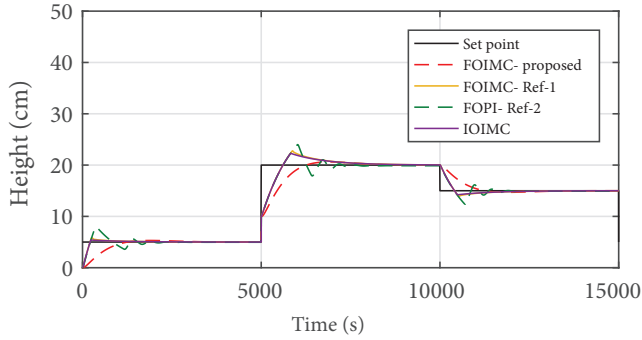
The FOIMC and the state of the art controllers are implemented on the cylindrical tank experimental setup. Figure 9a gives the experimental results with a step input. The experimental results show that FOIMC



(a) Comparison of the step responses

(b) Comparison of the regulatory responses

Figure 7. Simulation results-1



(a) Comparison of the servo responses

(b) Comparison of the robustness verification

Figure 8. Simulation results-2

Table 4. Time domain specifications- simulation.

Controller	t_r (sec)	t_s (sec)	M_p (%)	e_{ss}
FOIMC (proposed)	950	3000	6	0
FOIMC Ref-1	450	3000	25	0
FOPI Ref-2	450	3000	48	0
IOIMC	450	3000	18	0

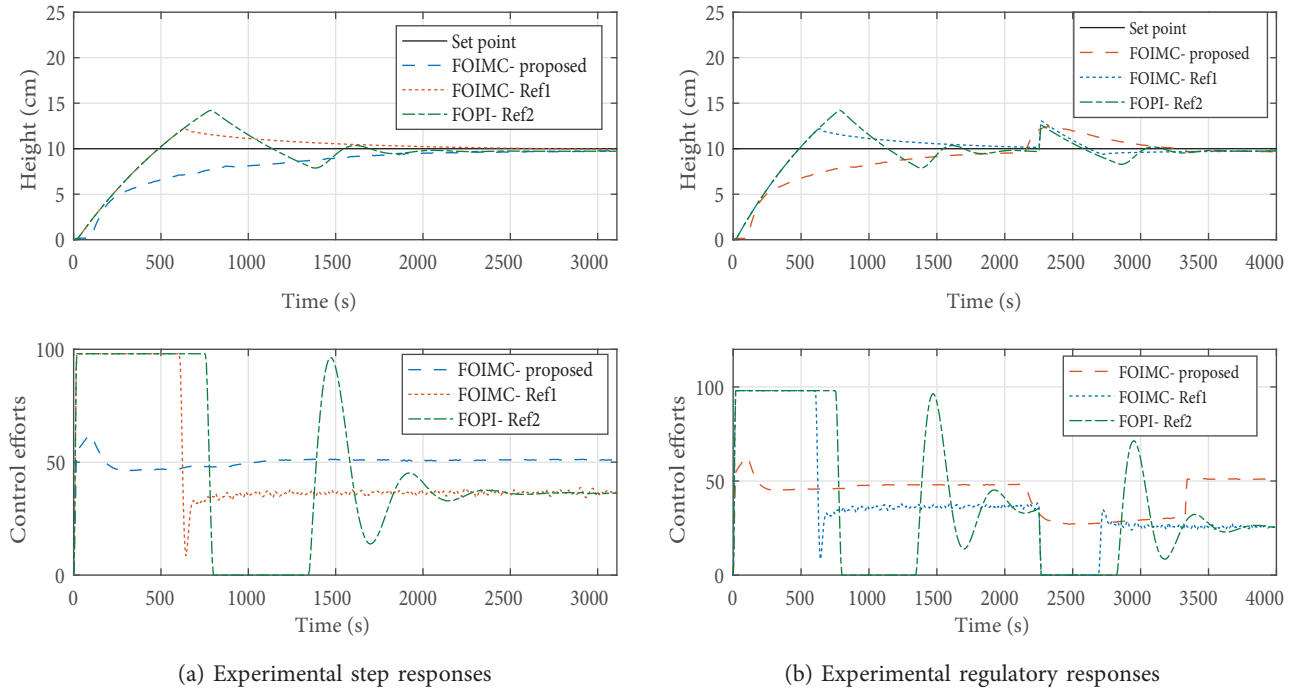


Figure 9. Experimental results.

has the lesser peak overshoot and lesser settling time, compared to Ref-1 and Ref-2. The control effort of the FOIMC is less compared to Ref-1 and Ref-2. To get the regulatory response, a disturbance is generated by changing the ball valve position at the outlet of the second tank. Figure 9b compares the experimental regulatory responses of the controllers and the control efforts. Figure 9b shows that the regulatory response of FOIMC quickly restores to the normal height of 10 cm from the disturbance. Figure 10 compares the experimental robustness verification responses of the controllers, and the control efforts. FOIMC gives satisfactory response at both the heights 10 cm and 20 cm. Table 5 shows time domain performance obtained from experimental results. The experimental results are in close agreement with the simulation results.

Table 6 shows the comparison of robust stability norms and fragility indices of the controllers. From Table 6, it is observed that the proposed controller is resilient, Ref-1 is nonfragile and Ref-2 is fragile when the controller parameters are varied by +20%. The proposed controller and Ref-2 have robust stability norms less than 0dB; hence, the proposed controller and Ref-1 are robustly stable. The Ref-1 has robust stability norm of 0.59 dB (> 0 dB); hence, Ref-1 is not robustly stable.

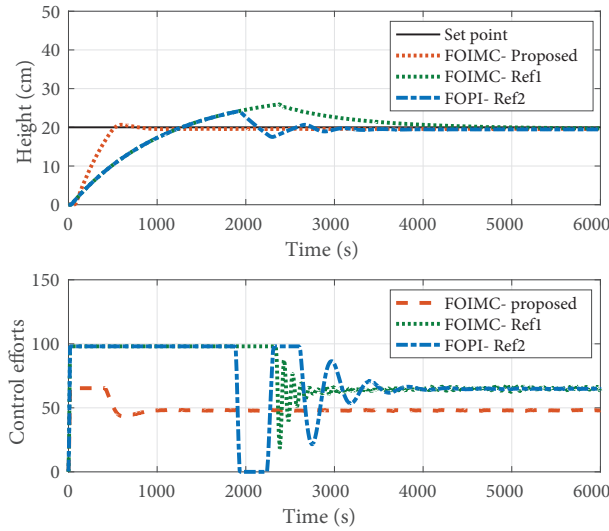


Figure 10. Comparison of the experimental robustness verification responses.

Table 5. Time domain specifications- experimental.

Controller	t_r (sec)	t_s (sec)	M_p (%)	e_{ss}
FOIMC (proposed)	1500	2250	0	0
FOIMC Ref-1	450	2500	25	0
FOPI Ref-2	450	2500	40	0

Table 6. Stability and robustness analysis.

Controller	$RFI_{\Delta 20}$	Stability H_{∞} norm (dB)
FOIMC (proposed)	0.00912	-18.45
FOIMC Ref-1	0.523	0.59
FOPI Ref-2	7.1	-9.67

6. Conclusion

This paper proposes a higher order fractional filter based FOIMC for the coupled tank system’s height control. PSO algorithm optimises the controller parameters of the FOIMC. Different filter combinations for the FOIMC are studied, and the proposed configuration gives better results for the level control of the coupled tank system. The performance of the proposed FOIMC is compared with state of the art. There is a 75% improvement in the peak overshoot of the proposed FOIMC, compared to Ref-1, 87.5 % compared to Ref-2 and 66.6 % compared to IOIMC. The FOIMC gave the least peak overshoot. The FOIMC and Ref-1 gave the same settling time and Ref-1 gave least settling time. The proposed controller gave higher rise time, and Ref-1, Ref-2 gave the same settling time. Also, the servo response and regulatory responses of the FOIMC are found to be better. The FOIMC has balanced the servo response, disturbance rejection, and robustness. FOIMC and the other controllers are implemented on the laboratory setup. The experimental results also confirm the superiority of the proposed FOIMC.

References

- [1] Sathish Kumar K, Kirubakaran V, Radhakrishnan TK. Real time modeling and control of three tank hybrid system. *Chemical Product and Process Modelling* 2017; 13 (1): 1-10. doi: 10.1515/cppm-2017-0016
- [2] Damrudhar, Tanti DK. Comparative performance analysis for two tanks liquid level control system with various controllers using MATLAB. *International Journal of Latest Trends in Engineering and Technology* 2016; 7 (2): 345-352. doi: 10.21172/1.72.555
- [3] Lakshmanprabu SK, Banu US. Adaptive multiloop IMC based PID controller tuning using bat optimisation algorithm for two interacting conical tank process. *International Journal of Advanced Intelligence Paradigm* 2019; 13 (3): 263-287. doi: 10.1504/IJAIP.2019.101979
- [4] Verma B, Padhy PK. Indirect IMC-PID controller design. *IET Control Theory Applications* 2019; 13 (2): 297-305. doi: 10.1049/iet-cta.2018.5454
- [5] Podlubny I, Dorack L, Kostial I. On fractional derivatives, fractional order dynamic systems and $PI^\lambda D^\mu$. In: *IEEE 1997 Decision and Control Conference, San Deogo, USA; 1997*; pp. 4985-4990. doi: 10.1109/CDC.1997.649841
- [6] Vinopraba T, Sivakumaran N, Narayanan S, Radhakrishnan TK. Design of internal model control based fractional order PID controller. *Journal of Control Theory Applications* 2012; 10: 297-302. doi: 10.1007/s11768-012-1044-4
- [7] Pachuari N, Yadav J, Rani A, Singh V. Modified fractional order IMC design based on drug scheduling for cancer treatment. *Computers in Biology and Medicine* 2019; 109: 121-137. doi: 10.1016/j.combiomed.2019.04.013
- [8] Maamar B, Rachid M. IMC PID fractional order filter controllers design for integer order systems. *ISA Transactions* 2014; 53 (5): 1620-1628. doi: 10.1016/j.isatra.2014.05.007
- [9] Baruah G, Majhi S, Mahanta C. Design of FOPI controller for time delay systems and its experimental validation. *International Journal of Automation and Computing* 2019; 16 (3): 310-328. doi: 10.1007/s11633-018-1165-4
- [10] Rayalla R, Ambati SR, Gara UB. An improved fractional filter fractional IMC-PID controller design and analysis for enhanced performance of non-integer order plus time delay processes. *European Journal of Electrical Engineering* 2019; 21 (2): 139-147. doi: 10.18280/ejee.210203
- [11] Nasir AW, Singh AK. IMC based fractional order controller for non-minimum phase system. In: *2015 Indian Control Conference, New Delhi, India 2015*; 25 (6): pp. 1-6. doi: 10.1109/INDICON.2015.7443593
- [12] Idamakanti K, Nasir AW, Singh AK. IMC based controller design for automatic generation control of multi-area power system via simplified decoupling. *International Journal of Control, Automation and Systems* 2018; 16 (3): 994-1010. doi: 10.1007/s12555-017-0362-1
- [13] Sonker B, Kumar D, Samuel P. Dual loop IMC structure for load frequency control issue of multi-area multi-sources power systems. *International Journal of Electrical Power & Energy Systems* 2019; 112: 476-494. doi: 10.1016/j.ijepes.2019.04.042
- [14] Chu M, Xu C, Chu J. Graphical IMC-PID tuning based on maximum sensitivity for fractional-order uncertain systems. In: *2018 IEEE International Conference on Automation, Electronics and Electrical Engineering 2018*; pp. 257-261. doi: 10.1109/AUTEEE.2018.8720809
- [15] Li D, He X, Song T, Jin Q. Fractional order IMC controller design for two-input-two-output fractional order system. *International Journal of Control, Automation and Systems* 2019; 17(4): 936-947. doi: 10.1007/s12555-018-0129-3
- [16] Muresan CI, Birs IR, Prodan O, Nascu I, Keyser RD. Approximation methods for FO-IMC controllers for time delay systems. In: *International Conference on Electrical Engineering and Green Energy; 2019*; pp. 1-6. doi: 10.1051/e3sconf/201911501003
- [17] Monje C, Chen YQ, Vinagre, Xue, Felieu V. *Fractional-order systems and controls: Fundamentals and applications*. London, UK: Springer-Verlag, 2010.

- [18] Teplijakov A, Petlenkov E, Belikov J. FOMCON: A MATLAB toolbox for fractional order system identification and control. *International Journal of Microelectronics and Computer Science*; 2011; 2 (2): 51-62.
- [19] Kennedy J, Eberhart R. Particle swarm optimisation. In: *International Conference on Neural Networks*; Perth, Australia; 1995. pp. 1942-1948.
- [20] Maiti D, Biswas S, Konar A. Design of a fractional order PID controller using particle swarm optimisation technique. In: *2nd National Conference on Recent Trends in Information Systems*; Coimbatore, India; 2008. arXiv:0810.3776
- [21] Xu L, Song B, Cao M, Xiao Y. A new approach to optimal design of digital fractional order PID controller. *NeuroComputing* 2019; 363: 66-77. doi: 10.1016/j.neucom.2019.06.059
- [22] Das S, Pan I, Das S, Gupta A. A novel fractional order fuzzy PID controller and its optimal time domain tuning based on integral performance indices. *Engineering Applications of Artificial Intelligence* 2012; 25 (2): 430-442. doi: 10.1016/j.engappai.2011.10.004
- [23] Zafer B, Oguzhan K. Fractional PID controllers tuned by evolutionary algorithms for robot trajectory control. *Turkish Journal of Electrical Engineering & Computer Sciences* 2012; 20 (1): 1123-1136. doi: 10.3906/elk-1102-1011
- [24] Mahdi S, Babak M, Gevork BG, Soodabeh S. Optimal fractional-order PID controller of inverter-based power plants for power systems LFO damping, *Turkish Journal of Electrical Engineering & Computer Sciences* 2020; 28: 485-499. doi: 10.3906/elk-1907-31
- [25] Tavazoei MS. Notes on integral performance indices in fractional order control systems. *Journal of Process Control* 2010; 20 (3): 285-291. doi: 10.1016/j.jprocont.2009.09.005
- [26] Castillo-Garcia FJ, Feliu-Batlle V., Rivas-Perez R. Time domain tuning of fractional order controllers combined with smith predictor for automation of water distribution in irrigation main channel pools. *Asian Journal of Control* 2013; 15 (3): 819-833. doi: 10.1002/asjc.558
- [27] Rajesh R. Optimal tuning of FOPID controller based on PSO algorithm with reference model for a conical tank system. *Springer Nature Applied Sciences* 2019; 1. doi: 10.1007/s42452-019-0754-3
- [28] Arya PP, Chakraborty S. IMC based fractional order controller design for specific non-minimum phase systems. In: *IFAC Conference on Advances in Proportional-Integral-Derivative Control*; Ghent, Belgium 2018; 51 (4): 4496-4509. doi: 10.1016/j.ifacol.2018.06.123
- [29] Komathi C, Umamaheswari MG. Design of GWO algorithm based FOPI controller for power factor correction in SMPS applications. *IEEE Transactions On Power Electronics* 2019; 35 (2): 2100-2118. doi: 10.1109/TPEL.2019.2920971
- [30] Rayalla R, Ambati SR, Gara BUB. Analytical design of fractional IMC filter PID control strategy for performance enhancement of cascade control systems. *International Journal of Systems Science* 2020; 1699-1713. doi: 10.1080/00207721.2020.1773571
- [31] Morrari M, Zafriou E. *Robust process control*. Englewood Cliffs, NJ, USA: Prentice Hall, 1989.
- [32] Alfaro VM, Vilanova R., *PID control in the third millennium 2012*. London, UK: Springer, 2012, pp. 349-380.